AIP | Journal of Applied Physics

The rigorous wave optics design of diffuse medium reflectors for photovoltaics

Albert Lin, Sze Ming Fu, Yan Kai Zhong, Chi Wei Tseng, Po Yu Chen, and Nyan Ping Ju

Citation: Journal of Applied Physics **115**, 153105 (2014); doi: 10.1063/1.4872140
View online: http://dx.doi.org/10.1063/1.4872140
View Table of Contents: http://scitation.aip.org/content/aip/journal/jap/115/15?ver=pdfcov
Published by the AIP Publishing

The rigorous wave optics design of diffuse medium reflectors for photovoltaics

Albert Lin,[a] Sze Ming Fu, Yan Kai Zhong, Chi Wei Tseng, Po Yu Chen, and Nyan Ping Ju
Department of Electronic Engineering, National Chiao-Tung University, Hsinchu 30010, Taiwan

(Received 6 February 2014; accepted 9 April 2014; published online 21 April 2014)

Recently, diffuse reflectors are being incorporated into solar cells, due to the advantage of no metallic absorption loss, higher reflectance, decent light scattering property by embedded TiO_2 scatterers, and the ease of fabrication. Different methods have been employed to analyze diffuse reflectors, including Monte Carlo method, N-flux method, and a one-dimensional approximation based on semi-coherent optics, and the calculated reflectance is around 80% by these methods. In this work, rigorous wave optics solution is used, and it is shown that the reflectance for diffuse medium mirrors can actually be as high as >99% over a broad spectral range, provided the TiO_2 scatterer geometry is properly optimized. The bandwidth of diffuse reflectors is un-achievable by other dielectric mirrors such as distributed Bragg reflectors or high index contrast grating mirror, using the same index contrast. Finally, it is promisingly found that even if the distribution of TiO_2 is random, the wide-band reflection can still be achieved for the optimized TiO_2 geometry. Initial experimental result is included in the supplementary material which shows the high feasibility of diffuse medium mirrors for solar cells. © *2014 AIP Publishing LLC*.
[http://dx.doi.org/10.1063/1.4872140]

I. INTRODUCTION

Diffuse reflectors have been shown to be of great interest for optoelectronic application,[1–6] due to its potential to replace conventional metallic mirrors[7–11] or conventional dielectric mirrors such as distributed Brag reflectors (DBR).[12] Recently, diffuse reflectors also find promising application in solar cells.[3–6] The advantage is that diffuse medium reflectors can replace the conventional metallic solar cell back reflectors to provide higher reflectance due to no metallic loss. Besides, the light trapping property can be enhanced by the embedded scatterers in the diffuse mirror. Compared to DBR, diffuse reflectors provide random light scattering where the direction of scattered solar photons is randomized. The randomization in light scattering is due to the embedded TiO_2 scatterers, and it is difficult to achieve the randomization using DBRs or other dielectric mirrors with well-defined geometries. This property leads to superior light trapping for diffuse medium reflectors. In addition, the processing of diffuse medium reflectors is lower-temperature, lower-cost, and higher-throughput than DBRs. Experimentally, sol-gel processes[13–15] or other wet chemical processes can be applied to realize such reflectors with relative ease, and no lithography and etching are needed. On the contrary, for distributed Brag reflectors the precise control of the layer thickness is necessary since the high reflectance (R) is achieved using constructive wave interference resulted from the reflection at the material interfaces.[16,17] Due to the above-mentioned advantages of diffuse mirrors, it is necessary to conduct a more detailed analysis on such reflectors to get insight on the design constraint, optimization, and the physics behind its high reflectance. In particular, the design and optimization on the geometry of the embedded TiO_2 scatterers is very critical. For the analysis of diffuse reflectors, several numerical methods have been previously applied including Monte Carlo method,[18] N-flux methods based on radiation transfer equations,[19–21] and one dimensional approximation based on semi-coherent optical modeling.[4] All of these works show the reflectance achieved is around 80%. Nevertheless, the analysis along the line of wave optics, in a three dimensional space, suggests that the reflectance can be increased to >99% over a broad spectral range if the optimization of the scatterer geometry is conducted. The lack of wave optics confirmation in the past is primarily due to the fact that the simulation of such a large structure takes very long CPU (central processing unit) runtime. Here, it is shown that, by using a frequency domain coupled wave method, the computation is still manageable. The result is then confirmed by a time domain method using finite difference time domain (FDTD) calculation.[22,23]

II. CALCULATION SET-UP AND METHODOLOGY

The real diffuse reflector (DR) consists of a low index host matrix material within which high index dielectric scatterers are embedded, as illustrated in Fig. 1. The scatterers are assumed to be cylindrical in shape. In experiment, cylindrical TiO_2 nano-rods have been extensively studied.[24–26] The TiO_2 scatterers can also be spheres or tubes, corresponding to nano-particles or nano-tubes. Based on our simulation results, the high reflection band can still be achieved for spherical scatterers as long as proper optimization of the scatterer geometry is conducted. The advantage of cylindrical shape over spherical shape is that there are two geometrical parameters, i.e., the cylinder height and diameter, to be adjusted instead of only one parameter, i.e., the sphere diameter. In previous methods, using Monte Carlo method,[18]

[a]hdtd5746@gmail.com

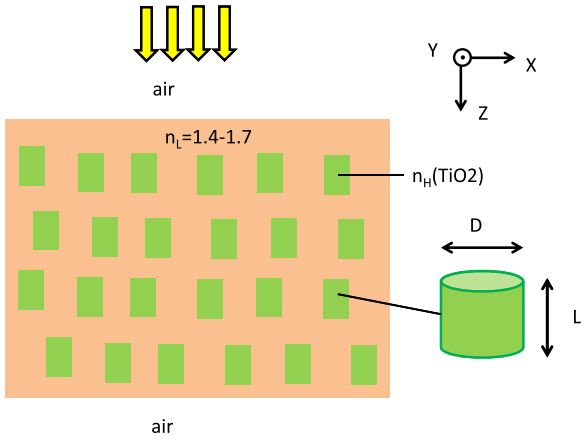

FIG. 1. The diffuse reflector with cylindrical TiO_2 scatterers. The low index (n_L) is usually varying between 1.4 and 1.7. The high index (n_H) is titanium dioxide (TiO_2).

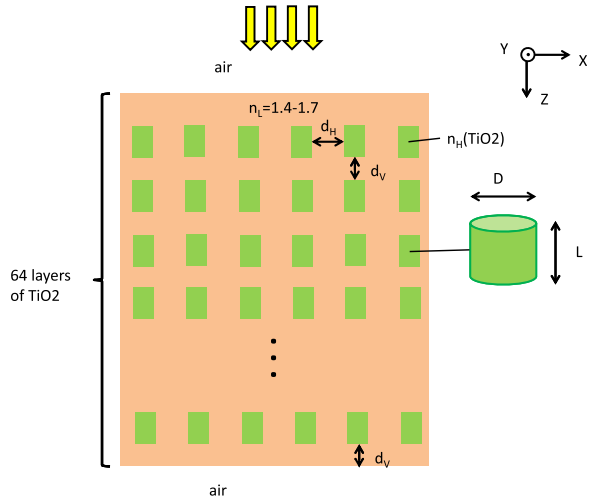

FIG. 2. Illustration of the *ordered* TiO_2 diffuse reflectors. The vertical spacing d_V is the same for each layer of the TiO_2 scatterers.

N-flux methods,[19–21] or one dimensional approximation using semi-coherent optics to simulate diffuse reflectors,[4] the shape of the scatterers does not have direct effect on the calculation result. Although it is going to be shown below that disorder is beneficial for a wide reflection band, it is still worth to point out that controlled and ordered TiO_2 nanorods in the low index materials is possible from fabrication point of view.[24,27]

The distribution of the dielectric scatterers might be disordered depending on the process methods. In this study, the simulation of diffuse reflectors is first conducted by calculating the reflectance of an ordered array of TiO_2 dielectric scatterers embedded in a low index host material. Afterward, the disorder is introduced in the z-direction (propagation direction), similar to the practice in literature.[4] In the most recent study in Ref. 4, one-dimensional (1D) approximation is used to transform 3D structure to 1D, and semi-coherent optics[4] is employed to calculate the reflectance. In this study, although the disorder is also introduced in z-direction, the simulation domain is still 3D. Therefore, the improvement over the past studies[4,18–21] on diffuse medium reflectors is in that wave optics is used here. In addition, the geometry of TiO_2 has significant effect on spectral response as a direct result of wave optics and due to the fact that three-dimensional (3D) nature of the structure is retained. The calculation methods are rigorously coupled wave analysis (RCWA)[22,28–30] and FDTD.[22,23] The setup for RCWA is not very different from usual grating simulations,[31] and the only difference is that here in z-direction (propagation direction) an ordered or disordered array of dielectric scatterers are stacked as illustrated in Figs. 2 and 4. The number of stacking is $N = 64$, and therefore in z-direction the structure is quite thick, similar to real diffuse reflectors.[3–6] For the disordered structure, the vertical spacing (z-direction) between the TiO_2 scattered is adjusted to achieve a wide reflectance band. The boundary condition for FDTD is perfectly matched layer (PML) at the top and the bottom boundaries (z-direction). Total field scattered field (TFSF) formulation is implemented above the diffuse reflector to simulate the incident field. The periodic boundary condition is applied at the x- and y-direction boundary in the three dimensional simulation domain. Since the CPU runtime for such a large structure is extremely long, the reflectance at selective wavelengths is calculated using FDTD to confirm the result by RCWA.

The material parameters of the host materials are normally low index with refractive index in the range of 1.4–1.7. It can be polymer-based for easier solution processing. It can also be oxide-based such as SiO_2 or silica glasses, which is more compatible to current silicon photovoltaic process technology. Nevertheless, oxide-based solution processes take more consideration. In fact, since for most of the polymer materials and oxide based materials, the refractive index are all around 1.5, the result presented here can apply well to a broad range of host materials and thus which low index material is used as an example does not really matter. The material refractive indices and extinction coefficients are from Rsoft material database.[22] The TiO_2 has a bandgap around 385 nm in the index data used here.

III. THE DIFFUSE REFLECTOR BASED ON ORDERED TiO_2 SCATTERERS

The simulation is carried out in a three-dimensional space, and thus the Fig. 2 is the cross-sectional view for the diffuse reflector. The TiO_2 scatterers are assumed to be cylindrical in shape, and the reason for choosing cylindrical scatterers is stated in the first paragraph of Sec. II. Polarization independence is achieved for normal incidence due to the rotational symmetry of the cylindrical scatterers. n_L used in the optimization for Fig. 3 is SiO_2 whose index is around 1.45 for the spectral range of interest here. In real diffuse reflectors, the randomly distributed TiO_2 scatterers where disorder exists in all of the three directions still makes a polarization-insensitive mirror due to the randomness. The TiO_2 scatterers are embedded in a low index host material. The d_V is the vertical spacing between TiO_2 scatterers and d_H is the horizontal spacing between TiO_2 scatterers. The diameter of the TiO_2 scatterers is D and the length is L. The number of TiO_2 layers actually depends on the thickness of the diffuse reflector, the length of the TiO_2 scatterers, and the vertical spacing d_V. The thickness of real diffuse

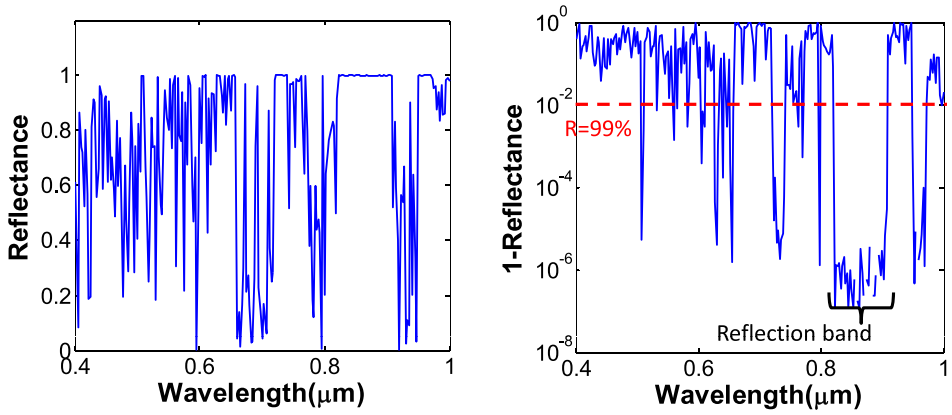

FIG. 3. (Left) the spectral reflectance (R) of the optimized *ordered* TiO_2 diffuse reflector. (Right) The semi-log plot of 1-Reflectance (R).

reflectors ranges from tens of micrometers to hundreds of micrometers. In this work, $N = 64$ is used for simulation, and therefore the thickness for the entire low index slab is $N \times (L + d_V) + d_V + d_V$. The separation between the first row of TiO_2 scatterers and the upper boundary of the low index slab is d_V, and the separation between the last row of TiO_2 scatterers and the lower boundary of the low index slab is also d_V. The D, L, d_V, and d_H determine pigment (TiO_2) volume concentration in the host low index material. By genetic algorithm (GA) optimization, the optimized geometry is $d_V = 0.188\,\mu m$, $d_H = 0.161\,\mu m$, $D = 0.396\,\mu m$, and $L = 0.2768\,\mu m$ for achieving maximized broadband reflectance. Fig. 3 plots the reflectance (R) of the optimized diffuse reflector with ordered TiO_2 scatterers. At the left of Fig. 3, the semi-log plot of 1-R is included to further show the relative value of high reflection in the spectral response. It should be pointed out that the bandgap of TiO_2 scatterers is around 385 nm in the index data used in this study and therefore the application of TiO_2 dielectric mirror is limited to the photon energy below its bandgap energy. The spectral reflectance in Fig. 3 cannot achieve very wide high reflectance band due to the fact that, for an ordered TiO_2 array, the constraint for constructive interference can only be fulfilled at a narrow range of wavelengths. The averaged value of 1-R in the reflection band (i.e., from 822.5 nm to 902.5 nm) is $1 - R_{avg} = 2.9264 \times 10^{-7}$. This is quite high reflectance, but the high reflection is limited to a narrow band range and thus may not meet the broadband requirement for photovoltaic application.

IV. THE DIFFUSE REFLECTOR BASED ON DISORDERED TiO_2 SCATTERERS

The simulation is also carried out in three-dimensional space, and thus Fig. 4 is still the cross-sectional view of a disordered diffuse reflector. The vertical spacing d_V is now separately adjusted to simulate the disorder in the distribution of TiO_2 scatterers. First, an optimized geometry will be discussed where the vertical spacing is selected by a genetic algorithm. Since, in some diffuse reflectors fabricated by sol-gel or other solution processes, the disorder may not be of a well-controlled nature, a randomly distributed TiO_2 diffuse reflector will be discussed later. In the case of a randomly distributed TiO_2, the vertical spacing $d_V(1)$, $d_V(2)$,…, $d_V(N)$ are randomly selected, and only d_H, D, and L can be optimized. Promisingly, it is found that even if the distribution of TiO_2 is random, the wide band reflection can still be achieved, and the spectral reflectance is only slightly degraded from the optimized disordered TiO_2 mirror. The dependence of spectral reflectance on the polarization and the incidence angle will be discussed later in Fig. 9. The reason for choosing cylindrical scatterers is stated in the first paragraph of Sec. II. In real diffuse reflectors, the disorder can exist in all of the three directions, but simulation of a three-dimensional disordered array will be computationally unmanageable based on our literature review. Simulating 1D disorder (z-direction), similar to the practice in Ref. 4, can capture the physics in diffuse reflectors. Based on the comparison between the ordered TiO_2 nano-particles in this work, the disorder in three directions is expected to enhance the performance of diffuse reflectors further. In Fig. 4, $d_V(1)$, $d_V(2)$,…, $d_V(N)$ are the vertical spacing between TiO_2 scatterers. Due to the fact that the disorder exists in the vertical direction, the d_V is now an array of length 64, and each element is denoted by $d_V(1)$, $d_V(2)$,…, $d_V(N)$. d_H is the horizontal spacing between TiO_2 scatterers. The diameter of cylindrical TiO_2 scatterers is D, and its length is L. n_L used

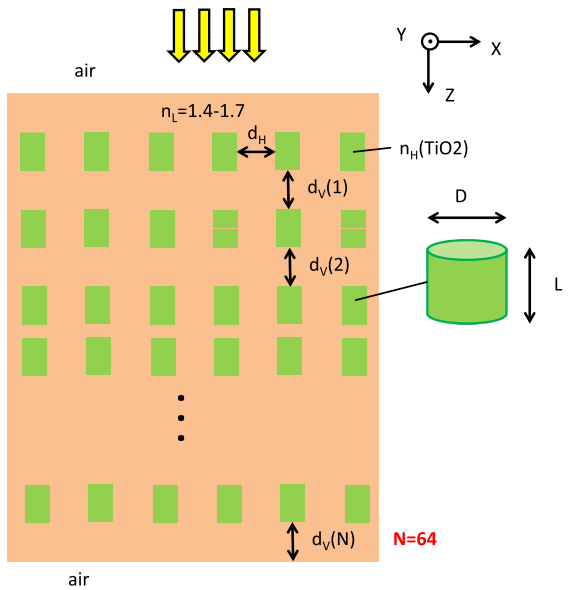

FIG. 4. Illustration of the *disordered* TiO_2 diffuse reflector. The vertical spacing d_V is different between each layer of the TiO_2 scatterers.

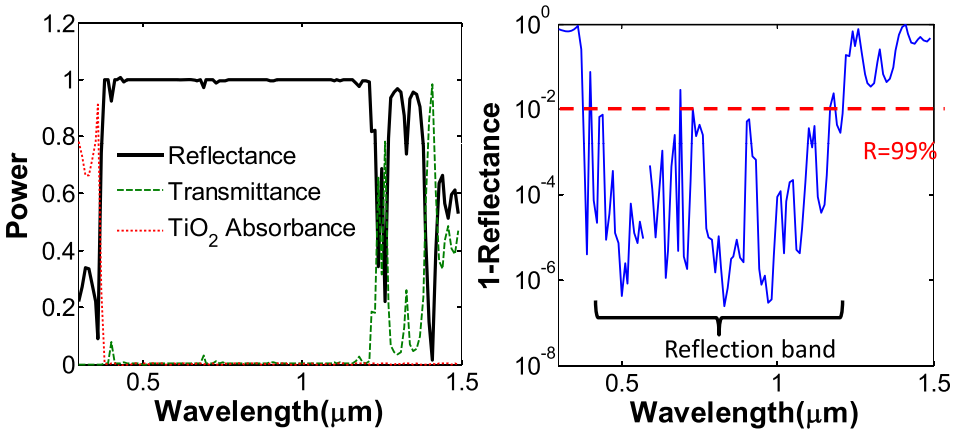

FIG. 5. (Left) the spectral reflectance for the *disordered* TiO_2 diffuse reflector. (Right) The semi-log plot of 1-Reflectance (R). The vertical spacings $d_V(1)$, $d_V(2)$,…, $d_V(N)$ between the disordered TiO_2 array are optimized with a genetic algorithm. $d_H = 25.4$ nm, $D = 0.229$ μm, and $L = 0.071$ μm.

in the optimization for Fig. 5 is SiO_2 whose index is around 1.45 for the spectral range of interest here.

For the GA optimized diffuse reflectors, the optimized geometry is $d_H = 25$ nm, $D = 0.229$ μm, $L = 0.071$ μm. d_V is now an array with 64 elements. Its value falls between 10 nm and 300 nm and is optimized by genetic algorithm. Since this is a long list, the values are not included here. The spectral response in Fig. 5 shows the reflectance, absorbance, and transmittance for the TiO_2 diffuse reflector. At the left of Fig. 5, the semi-log plot of 1-R is included to further show the relative value of high reflection in the spectral response. It can be seen from the semi-log plot that within the high reflection band, the most of the reflectance values are above 0.99. The value of $1 - R_{avg}$ is 0.0087 within the high reflection band (i.e., 387.5 nm–1202.5 nm). The value of $1\text{-}R_{avg}$ is higher than the ordered TiO_2 scatterers, reflecting that the spectral reflectance is compromised over broader wavelength range. This is in contrast to the narrow band sharp reflectance of an ordered diffuse mirror. Nonetheless, it should be pointed out that, at most of the spectral points in the reflection band, $R > 0.99$ is still achieved for the disordered mirror. Therefore, disordered TiO_2 mirrors can be very promising for many optoelectronic applications if a broadband response is needed. The reflectance drops significantly below $\lambda = 400$ nm due to severe TiO_2 absorption. In addition, the reflection band covers from $\lambda = 400$ nm to $\lambda = 1200$ nm, which is essentially the whole light trapping regime of interest for solar cells. Therefore, using diffuse TiO_2 mirrors as the reflectors for future photovoltaics can lead to lower cost,[3–6] higher reflectance due to no metallic absorption loss, and very wide reflection band. DBR with the same index contrast (n_H is TiO_2 and $n_L = 1.45$) can only cover from $\lambda = 400$ nm to $\lambda = 630$ nm for a 10-pair DBR. Increasing the number of pairs only sharpens the response but does not increase the bandwidth. In order to verify the result using RCWA, calculation using FDTD is conducted here to verify the result. It can be seen in Fig. 6 that within the entire high reflection band, FDTD simulation also shows very high reflectance close to 1 consistent with the RCWA calculation. It should be pointed out that the simulation domain in this study is extremely large since it is three-dimensional and contains $N = 64$ layers of TiO_2 scatterer arrays. The FDTD verification is an extremely time consuming task and therefore frequency domain methods are critically needed for

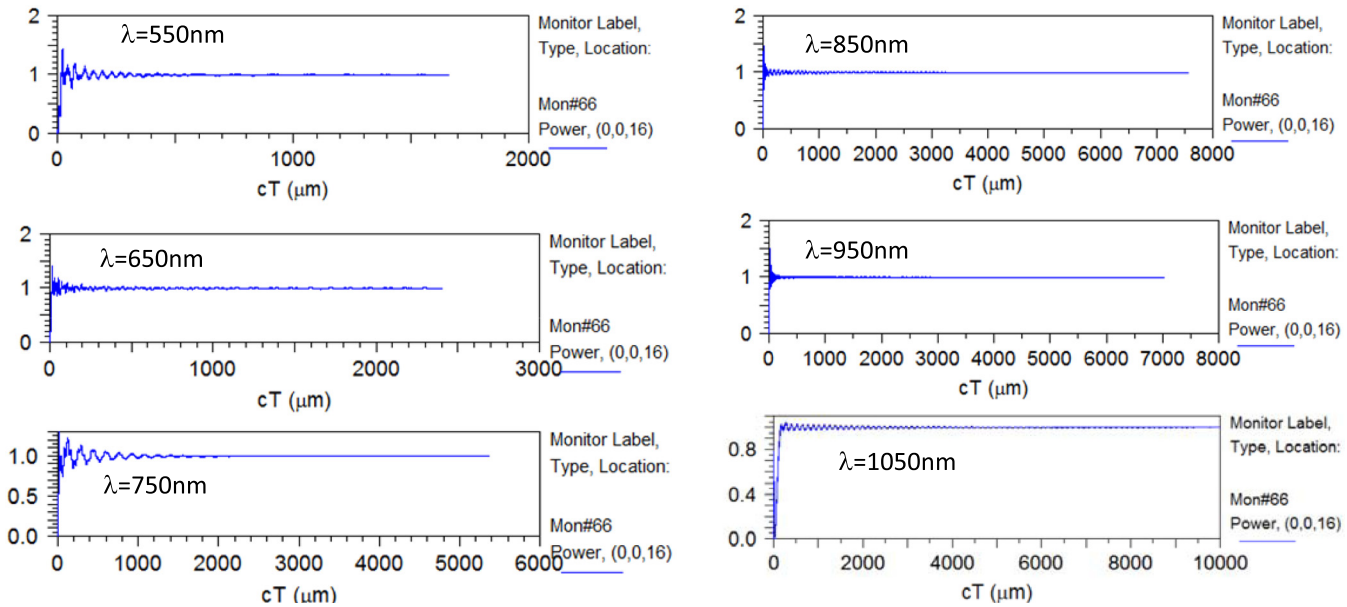

FIG. 6. The FDTD verification of the high reflectance (R) for the spectral reflectance in Fig. 5.

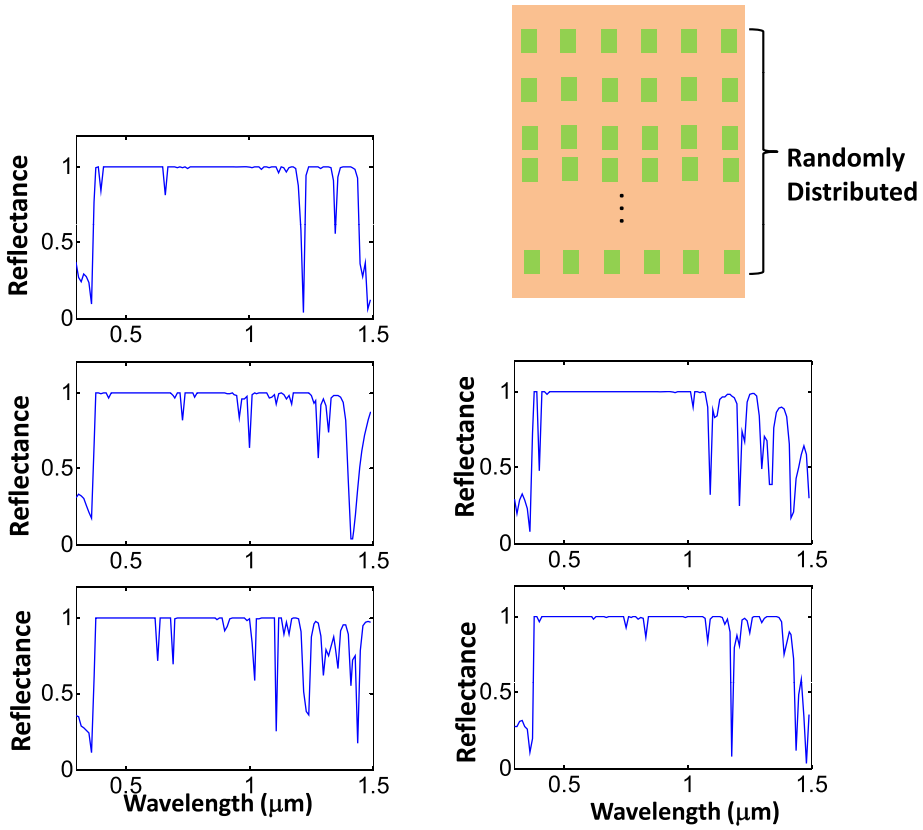

FIG. 7. The spectral reflectance of the *non-optimized randomly* disordered TiO_2 diffuse reflectors. In this case, the vertical spacings $d_V(1)$, $d_V(2)$,…, $d_V(N)$ between TiO_2 scatterers are random. This figure includes five runs for the random TiO_2 reflectors.

future diffuse reflector design and optimization based on wave optics.

One key issue for the disordered diffuse mirror is that, in real practice, the optimized spacing may not be achievable, depending on process control. In order to show that the superior performance of the disordered TiO_2 mirrors will not disappear even if the disorder is not optimized, spectral reflectance is calculated for several runs for a randomly distributed TiO_2 mirrors. In this case, $d_V(1)$, $d_V(2)$,…,$d_V(N)$ are randomly generated between 10 nm and 300 nm, and they are not optimized by the genetic algorithm optimization. D, L, d_H are kept the same as in Fig. 5. Fig. 7 shows the resulting spectral reflectance where the vertical separation between each TiO_2 scatterers is determined randomly based on a computerized random number generator. Clearly, the spectral response still shows satisfactory broadband reflectance where the high reflectance is only slightly degraded at certain wavelengths, compared to the optimized TiO_2 diffuse reflector. This is a promising finding since, in practice, the TiO_2 scatterers are likely to be distributed randomly in the low index material. While the randomly distributed TiO_2 mirrors can still provide broadband high reflectance even without optimization, it is feasible to use TiO_2 diffuse reflectors to replace the conventional DBRs or metallic reflectors.

The geometry of embedded TiO_2 nano-particles is critical, as can be seen from Fig. 8. Improperly chosen geometry will generally lead to degraded reflectance, and this reflects the importance of systematic optimization. In most of the current initial experimental effort on using diffuse medium reflector for solar cells, optimization of the scatterer geometry is not considered. In fact, the optimization of the scatterer geometry is possible only if wave optics is employed to describe the photon scattering phenomenon of the dielectric scatterers accurately. For solar cell broadband application, non-optimized TiO_2 scatterer geometry is detrimental since the reflection band should be as wide as possible to cover the

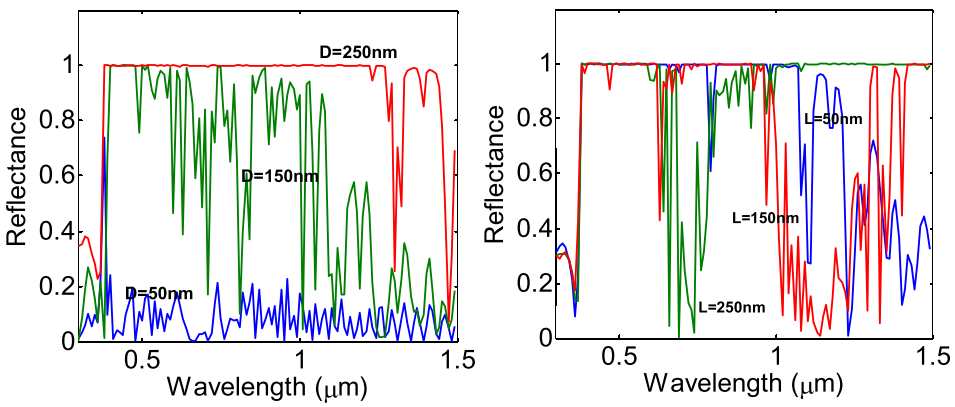

FIG. 8. The spectral reflectance of diffused medium mirror with various TiO_2 scatterer geometry. L is the cylindrical scatterer length, and D is the cylindrical scatter diameter. D and L are labeled in figure and $d_H = 25.4$ nm. The $d_V(1)$, $d_V(2)$,…, $d_V(N)$ are the same as in Fig. 5.

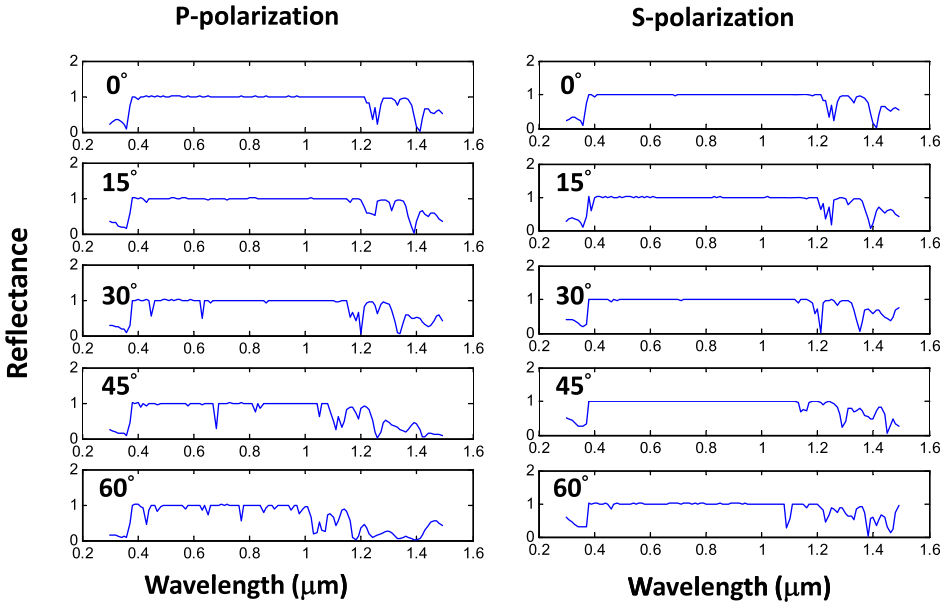

FIG. 9. The polarization and incidence angle dependence for the diffuse white paint reflector. The geometry is from Fig. 5.

entire solar spectrum. The initial experimental result for white-paint diffuse reflector is included in the supplementary material for review,[35] and it is observed that the high reflectance of white diffuse medium can indeed enhance the photocurrent generation.

Fig. 9 shows the angular responses for the diffuse white paint reflectors with the geometry the same as the mirror in Fig. 5. A broadband, omnidirectional, and polarization insensitive mirror is important for solar cells since the sun is traversing during a day and the solar photons are generally randomly polarized. From the reflectance plots in Fig. 9, it can be seen that the broadband reflectance exists for both s- and p-polarizations. This is due to the random light scattering behavior contributing to the high reflectance is itself relatively polarization independent. This kind of feature is very difficult to achieve using other dielectric or metallic mirrors since their well-defined geometry inevitably leads to strong polarization dependence. For oblique incidences, it can be seen from Fig. 9 that the reflection bandwidth is gradually reduced when solar photons are incident with larger angles. Nonetheless, the reflection bandwidth still covers the $\lambda = 400\,\text{nm}$–$\lambda = 1000\,\text{nm}$ spectral range which is of interest for silicon solar cell application. It should also be pointed out that the bandwidth reduction phenomenon is much alleviated compared to many reflection mirrors such as high index grating.[32] This is partly due to the random light scattering nature of the diffuse medium reflectors where the high reflectance does not count on the resonance condition at a specific incidence angle. The other reason for the superior angular performance is due to the thick dimension of the diffuse medium reflectors and therefore the photons can still encounter a sufficient number of scattering for oblique incident angles.

V. FIELD PROFILES AND THE MECHANISM FOR HIGH REFLECTANCE

Figs. 10 and 11 show the field profiles for the ordered and the disordered diffuse reflectors, respectively, for the spectral response in Figs. 3 and 5. From the field plots, it can be seen that at high reflectance wavelengths ($\lambda = 860\,\text{nm}$ in Fig. 10 and $\lambda = 800$ nm in Fig. 11), no field exists deep inside the diffuse reflectors for both cases. On the other hand, at low reflectance wavelengths, photons deeply

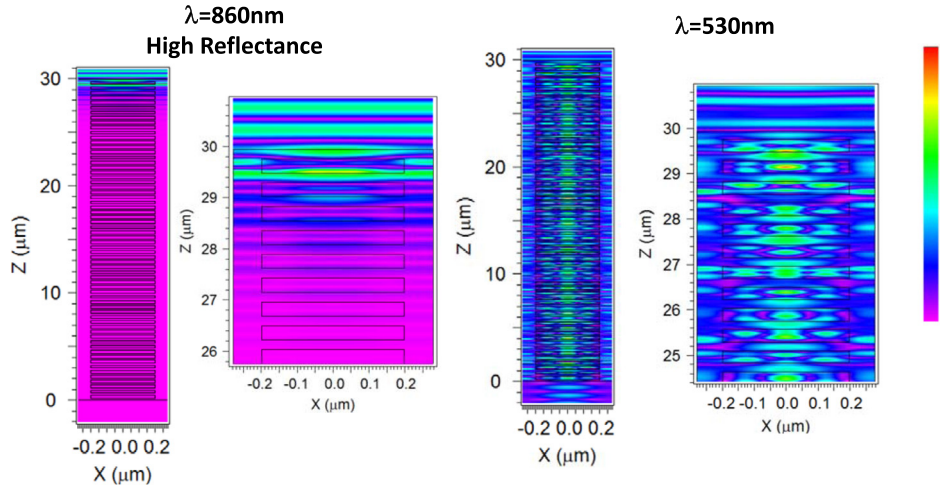

FIG. 10. The field plot of the *ordered* TiO_2 diffuse reflector whose spectral response appears in Fig. 3. The left field profile is for high reflectance ($\lambda = 830\,\text{nm}$).The right field profile is for wavelength ($\lambda = 530\,\text{nm}$) outside high reflectance band.

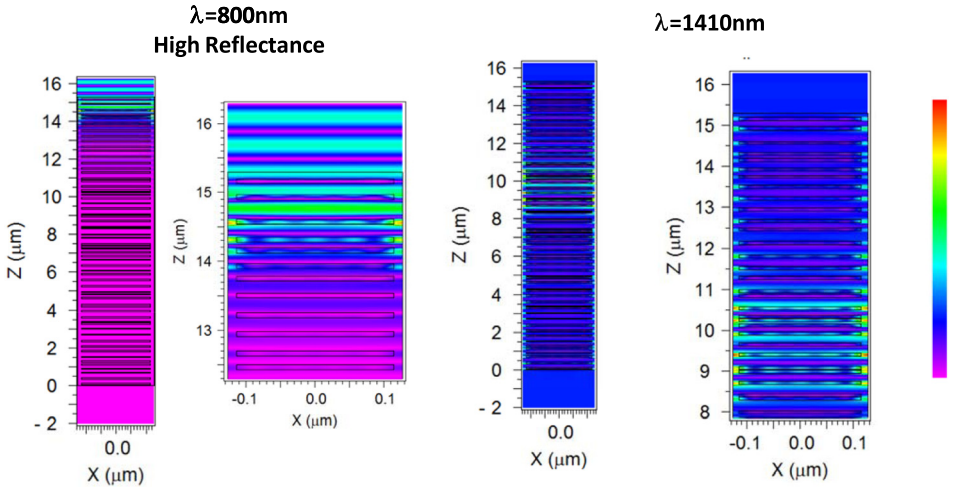

FIG. 11. The field plot of the *disordered* TiO_2 diffuse reflector whose spectral response appears in Fig. 5. The left field profile is for high reflectance ($\lambda = 800$ nm).The right field profile is for wavelength ($\lambda = 1410$ nm) outside high reflectance band.

penetrate through the entire structures. This observation applies to both of the ordered and the disordered structures. The zoom-in of the field profiles at the upper part of the plots reveals the scattering phenomenon initiated by the TiO_2 scatterers. In fact, the structure can be regarded as a photonic crystal with finite thickness where z-direction is the finite thickness direction and x- and y-direction are infinitely extended. For wavelengths leading to low reflectance, the incident photons actually couple into the guided modes. On the other hand, if the incident wavelengths fall into the photonic bandgap, high reflectance is resulted. The structure can also be regarded as a waveguide array in z-direction.[31,33,34] The successive reflection of the waveguide modes can then be added up, and a high reflectance band can be resulted if constructive interference is achieved. In a more conceivable picture, the physics of high reflectance can be explained by the successive photon scattering by TiO_2 scatterers. In the case of the ordered TiO_2 arrays, the reflected waves can be added up coherently at certain wavelengths and thus result in discrete high reflectance bands. Nonetheless, since the constructive interference, for an ordered arrays of TiO_2, cannot exist at a wide range of wavelengths, broad reflection band is difficult to achieve even after geometry optimization. In the case of disordered TiO_2 arrays, the disorder results in random phase for scattered photons. The random phase is beneficial for the broader bandwidth of high reflectance, due to the fact that the condition for the constructive interference is now easier to fulfill by the more flexibly placed TiO_2 scatterers. In this study, $N = 64$ layers of TiO_2 arrays are used for the calculation of the diffuse reflectors because for real diffuse reflectors the thickness is around ten to several hundred micrometers.[3–6] In fact, the number of layers can be reduced while the reflection band can still be maintained, provided the optimization is properly conducted.

VI. CONCLUSION

While the past analysis along the line of semi-coherent or geometrical optics predicts the broadband reflectance of diffuse medium reflectors is around 80%, the >99% broadband reflectance for diffuse reflectors is confirmed using wave optics in three dimensional spaces for the first time. The geometry of the TiO_2 is shown to be critical to provide the desired the broad reflection band. The bandwidth achieved by the disordered TiO_2 diffuse reflector is much wider than the reflection band of 230 nm achieved by DBR using the same index contrast (n_H is TiO_2 and $n_L = 1.45$). As far as the solar cell application is concerned, the diffuse mirror can cover the entire solar spectrum of interest from 400 nm to 1000 nm while it provides the advantage of low cost, low temperature, high throughput processing, compared to metallic back reflectors. The physics of high reflectance in diffuse reflectors is identified to be the successive photon scattering by TiO_2 scatterers, by observing the field distribution in wave optics simulation. In the case of an ordered TiO_2 reflector, the reflected waves can be added coherently at certain wavelengths and this results in discrete high reflectance bands. In the case of a disordered TiO_2 reflector, the random phase can lead to a broader bandwidth due to the compromise over the entire spectral range. The preliminary experimental result, confirming the usage of diffuse medium reflectors for photovoltaics, is included in supplementary material.[35]

ACKNOWLEDGMENTS

This work was funded by National Science Council (NSC), Taiwan, under Grant No. NSC 102-2221-E-009-121.

[1]J. K. Kima, H. Luo, Y. Xi, J. M. Shah, T. Gessmann, and E. F. Schubert, J. Electrochem. Soc. **153**(2), G105–G107 (2006).
[2]J. Chen, A. Hangauer, R. Strzoda, and M.-C. Amann, Appl. Phys. B **100**(2), 417–425 (2010).
[3]A. Goetzberger, *Paper Presented at the 15th IEEE Photovoltaic Specialist Conference, Kissimmee, Florida, USA, 1981*.
[4]B. Lipovšek, J. Krč, O. Isabella, M. Zeman, and M. Topič, J. Appl. Phys. **108**(10), 103115 (2010).
[5]O. Berger, D. Inns, and A. G. Aberle, Sol. Energy Mater. Sol. Cells **91**(13), 1215–1221 (2007).
[6]J. Meier, U. Kroll, J. Spitznagel, S. Benagli, T. Roschek, G. Pfanner, C. Ellert, G. Androutsopoulos, A. Hugli, M. Nagel, C. Bucher, L. Feitknecht, G. Buchel, and A. Buchel, *paper presented at the 31th IEEE Photovoltaic Specialist Conference, Orlando, Florida, USA, 2005*.
[7]H.-Y. Lin, Y. Kuo, C.-Y. Liao, C. C. Yang, and Y.-W. Kiang, Opt. Express **20**(S1), A104–A118 (2012).
[8]C. Battaglia, C.-M. Hsu, K. S. Derstrom, J. Escarre, F.-J. Haug, M. Charriere, M. Boccard, M. Despeisse, D. T. L. Alexander, M. Cantoni, Y. Cui, and C. Ballif, ACS Nano **6**(3), 2790–2797 (2012).

[9]U. W. Paetzold, E. Moulin, B. E. Pieters, R. Carius, and U. Rau, Opt. Express **19**(S6), A1219–A1230 (2011).
[10]U. W. Paetzold, E. Moulin, D. Michaelis, W. Bottler, C. Wachter, V. Hagemann, M. Meier, R. Carius, and U. Rau, Appl. Phys. Lett. **99**(18), 181105 (2011).
[11]K. Söderström, F.-J. Haug, J. Escarré, O. Cubero, and C. Ballif, Appl. Phys. Lett. **96**(21), 213508 (2010).
[12]P. Bermel, C. Luo, L. Zeng, L. C. Kimerling, and J. D. Joannopoulos, Opt. Express **15**(25), 16986–17000 (2007).
[13]C. J. Brinker and G. W. Scherer, *Sol-Gel Science*, 1 ed. (Academic Press, San Diego, CA, 1990).
[14]C. J. Brinker, A. J. Hurd, P. R. Schunk, C. S. Ashely, R. A. Cairncross, J. Samuel, K. S. Chen, C. Scotto, and R. A. Schwartz, in *Metallurgical and Ceramic Protective Coatings*, edited by K. Stern (Chapman & Hall, London, 1996), pp. 112–151.
[15]*The Springer International Series in Engineering and Computer Science*, edited by L. C. Klein (Springer, Berlin, 1994).
[16]P. Bhattacharya, *Semiconductor Optoelectronic Devices*, 2nd ed. (Prentice-Hall, Upper Saddle River, NJ, 2006).
[17]S. L. Chuang, *Physics of Photonic Devices*, Wiley Series in Pure and Applied Optics, 2nd ed. (Wiley, New York, 2009).
[18]P. Nitz, J. Ferber, R. Stangl, H. R. Wilson, and V. Wittwer, Sol. Energy Mater. Sol. Cells **54**(3), 297–307 (1998).
[19]W. E. Vargas, A. Amador, and G. A. Niklasson, Opt. Commun. **261**(1), 71–78 (2006).
[20]W. E. Vargas, P. Greenwood, J. E. Otterstedt, and G. A. Niklasson, Sol. Energy **68**(6), 553–561 (2000).
[21]J. E. Cotter, J. Appl. Phys. **84**(1), 618–624 (1998).
[22]Rsoft, *Rsoft CAD User Manual*, 8.2 ed. (Rsoft Design Group, New York, 2010).
[23]Synopsys (2005), pp. 78–79.
[24]Y. Han, C. Fan, G. Wu, H.-Z. Chen, and M. Wang, J. Phys. Chem. C **115**, 13438–13445 (2011).
[25]A. Sadeghzadeh-Attar, M. S. Ghamsari, F. Hajiesmaeilbaigi, and S. Mirdamadi, Semicond. Phys., Quantum Electron. Optoelectron. **10**(1), 36–39 (2007).
[26]L. Miao, S. Tanemura, S. Toh, K. Kaneko, and M. Tanemura, J. Mater. Sci. Technol. **20**(S1), 59–62 (2004).
[27]C. Y. Kuo, W. C. Tang, C. Gau, T. F. Guo, and D. Z. Jeng, Appl. Phys. Lett. **93**, 033307 (2008).
[28]M. G. Moharam and T. K. Gaylord, J. Opt. Soc. Am. A **3**(11), 1780–1787 (1986).
[29]M. G. Moharam and T. K. Gaylord, J. Opt. Soc. Am. **71**(7), 811–818 (1981).
[30]H. Kogelnik, Bell Syst. Tech. J. **48**, 2909–2947 (1969).
[31]C. F. R. Mateus, M. C. Y. Huang, Y. Deng, A. R. Neureuther, and C. J. Chang-Hasnain, IEEE Photonics Technol. Lett. **16**(2), 518–520 (2004).
[32]S. Boutami, B. B. Bakir, H. Hattori, X. Letartre, J.-L. Leclercq, P. Rojo-Romeo, M. Garrigues, C. Seassal, and P. Viktorovitch, IEEE Photonics Technol. Lett. **18**(7), 835–837 (2006).
[33]V. Karagodsky and C. J. Chang-Hasnain, Opt. Express **20**(10), 10888–10895 (2012).
[34]V. Karagodsky, F. G. Sedgwick, and C. J. Chang-Hasnain, Opt. Express **18**(16), 16973–16988 (2010).
[35]See supplementary material at http://dx.doi.org/10.1063/1.4872140 for preliminary experimental verification of diffuse medium mirrors for solar cells.